

Strong emission from As monolayers in AlSb

E. R. Glaser, T. A. Kennedy, B. R. Bennett, and B. V. Shanabrook

Naval Research Laboratory, Washington, D.C. 20375-5347

(Received 8 June 1998)

Strong photoluminescence (PL) bands between 1.41 and 1.62 eV have been observed from superlattices (SL's) composed of fractional or single monolayers (ML) of AlAs separated by 22–49 ML of AlSb. The emission exhibits a weak dependence on the SL period but shifts significantly to higher energy with decreasing AlAs thickness. Optically detected magnetic-resonance (ODMR) experiments at 24 GHz on the 1.45-eV PL from the SL's with ~ 1 ML of AlAs reveal $S = \frac{1}{2}$ electron spin transitions with $g_{\parallel} = (1.916-1.923) \pm 0.002$ and $g_{\perp} = (1.934-1.944) \pm 0.002$ split by an exchange interaction (Δ) of $(3.4-8.0) \pm 0.2 \mu\text{eV}$ with holes derived from the $J_z = \pm \frac{3}{2}$ valence band. Exchange-split electron resonances with $g_{\parallel} = 1.868 \pm 0.002$ and $g_{\perp} = 1.882 \pm 0.002$ and $\Delta = 19.5 \pm 0.5 \mu\text{eV}$ were detected on the 1.62-eV band from a sample with 31 ML of AlSb and 0.27 ML of AlAs. The PL and ODMR results can be understood using a type-II band lineup with the electron localized at the AlAs ML and the hole excluded to the AlSb layers. The electron g values and the strength of the exchange interaction reflect the degree of wave-function penetration into the adjacent AlSb barriers. The weakly bound excitons are localized at fluctuations along the AlSb/AlAs interfaces. [S0163-1829(99)00303-3]

I. INTRODUCTION

Large sheet charge densities are desirable for optimal performance of high-speed field-effect transistors (FET's) employing an InAs channel and AlSb barriers. One method to enhance electron concentrations is the addition of a monolayer of AlAs near the center of the top AlSb barrier layer.^{1,2} This "As-soak" technique gives as large as a fourfold increase in the carrier concentration compared to that for undoped structures. However, the origin of the carriers has not been established. One group¹ suggested As_{Al} antisites as the donor.

In this paper we have grown a set of superlattices (SL's) by molecular-beam epitaxy (MBE). Each period consists of 0.3–1 ML of AlAs separated by 22–49 ML of AlSb. Photoluminescence (PL) and optically detected magnetic resonance (ODMR) at 1.6 K were employed to identify the donors produced by the As sheets. It was anticipated that the dopants would be revealed in these test structures through their participation in one or more optical processes and that information on their chemical nature would be obtained from the detection of magnetic resonance.

Unexpectedly, very strong PL bands were found. The PL depends weakly on the SL period, but depends strongly on the AlAs thickness. All these samples exhibit strong ODMR, which is very similar to that found on excitonic emission from type-II GaAs/AlAs multiple quantum wells (MQW's).³⁻⁵ The energy of the emission, the electron g values, and the strength of the exchange interaction can be understood from the type-II band structure predicted using the band offsets for an AlSb/AlAs heterojunction⁶ with the electron confined largely in the AlAs ML and the hole excluded to the adjacent AlSb layers. These excitons are weakly bound to fluctuations at the AlSb/AlAs interfaces. Thus, this strong PL does not appear to involve the donorlike defects produced by the "As-soak" technique.

II. EXPERIMENTAL DETAILS

The PL and ODMR experiments were performed on a set of $[(\text{AlSb})_x(\text{AlAs})]_{120}$ ($x = 22-49$ ML) superlattices grown on GaAs (001) substrates by MBE at 500 °C, the same temperature as employed for the growth of InAs/AlSb FET's.² A 1- μm AlSb buffer layer was grown prior to deposition of the SL. The AlAs monolayer was formed as follows. The bottom AlSb layer was terminated with a ML of Al. Next, the surface was exposed to a beam of As_4 for 7 s. This was followed by an additional ML of Al. The Sb shutter was then reopened and the top AlSb layer was grown. After 120 periods of this procedure, a 50 Å GaSb cap layer was deposited. A superlattice consisting of 31 ML of AlSb and 0.27 ML of AlAs was also grown as described above, except the Al-terminated surfaces were exposed to Sb_4 for 2 s and As_4 for 2 s. (The fractional ML can be modeled as one ML of an $\text{AlAs}_{0.27}\text{Sb}_{0.73}$ alloy.) In addition, superlattices were grown uniformly doped with either Be (an acceptor) or Ga (an isoelectronic impurity) at concentrations of $\sim 3 \times 10^{16} \text{ cm}^{-3}$ as other methods to induce recombination involving the unknown donor species. Finally, a 4- μm AlSb/GaAs reference sample was studied.

The superlattices were characterized by single-crystal x-ray diffraction using the (004) reflection to obtain the out-of-plane lattice constants. The spectrum found for the $[(\text{AlSb})_{31}(\text{AlAs})_{1.06}]_{120}$ SL is shown in Fig. 1. The narrow lines and multiplicity of satellite peaks indicate the high quality of these samples. The structural parameters of the SL's determined from analyses of the x-ray data are given in Table I. The superlattices are strained coherently to the AlSb buffer layers with average AlSb and AlAs layer thicknesses in good agreement with the intended values. In addition, the small shift of the x-ray peak associated with the AlSb buffer layer from that for unstrained AlSb reveals that the buffer layers are not fully relaxed but are under an average in-plane biaxial compression of $0.08 \pm 0.02\%$. One consequence of this strain will be discussed later in the paper.

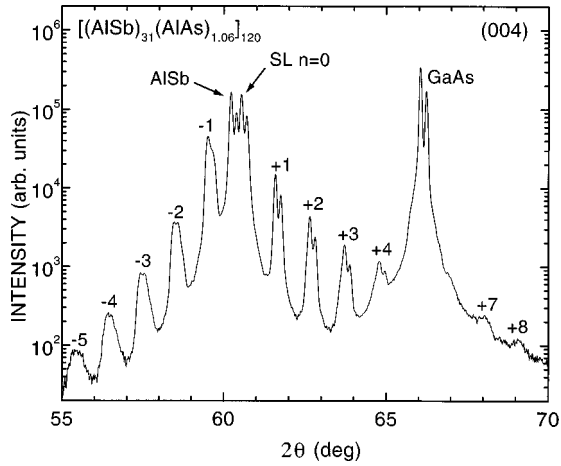


FIG. 1. X-ray diffraction θ - 2θ scan showing the (004) reflection for the $[(\text{AlSb})_{31}(\text{AlAs})_{1.06}]_{120}$ superlattice. The $(K\alpha_1-K\alpha_2)$ splittings are observed for several satellites. The SL was deposited on a GaAs substrate with a $1\text{-}\mu\text{m}$ AISb buffer layer.

The PL at 1.6 K from the AISb/AlAs superlattices and the AISb epitaxial layer was excited by the 488-nm line from an Ar^+ laser in the backscattering geometry with the incident light nearly along the [001] growth direction. Searches for emission between 0.7 and 1.7 eV were made using a liquid-nitrogen-cooled Ge photodiode, a Si photodiode, and a GaAs photomultiplier. The PL was dispersed with a 0.25-m double-grating spectrometer.

The ODMR was detected as the change in the total intensity of the strong PL, which was coherent with on-off amplitude modulation at 3 kHz of 50 mW of microwave power at 24 GHz. The ODMR was performed in the Voigt geometry with the dc magnetic field (\mathbf{B}), the wave vector of the excitation (\mathbf{k}), and the microwave magnetic field ($\mathbf{H}_{\mu\text{-wave}}$) mutually orthogonal. The magnetic field was provided by a 9-in-pole-face electromagnet. Photoexcitation power densities near 30 mW/cm^2 gave good signal-to-noise ratios. The PL was detected by the Si photodiode. A Schott RG830 filter was placed in front of the detector when necessary to block residual band-edge emission from the GaAs substrate. ODMR was also obtained with \mathbf{B} rotated in the $(1\bar{1}0)$ plane to obtain symmetry information.

III. RESULTS AND ANALYSES

A. PL

The photoluminescence from two AISb/AlAs superlattices and from the AISb reference sample is shown in Fig. 2.

TABLE I. Structure, emission energies, and magnetic-resonance parameters for $[(\text{AlSb})_M(\text{AlAs})_N]_{120}$ superlattices investigated in this work.

Structure		Emission			Fine structure			
AlSb (ML)	AlAs (ML)	ZPL Energy (eV)	Electron		Exchange splitting (Δ) (μeV)	Hole		
			g_{\parallel}	g_{\perp}		g_{\parallel}	g_{\perp}	
31 (1)	0.27 (0.05)	1.613 (0.001)	1.868 (0.002)	1.882 (0.002)	19.5 (0.5)			
31 (1)	1.06 (0.05)	1.417 (0.001)	1.922 (0.002)	1.939 (0.002)	3.7 (0.2)	2.8 (0.1)	~ 0	
22 (1)	0.92 (0.05)	1.452 (0.001)	1.923 (0.003)	1.944 (0.003)	8.0 (0.2)			
25(1) ^a	0.95 (0.05)	1.467 (0.001)			7.4 (0.2)			
49 (1)	0.88 (0.05)	1.454 (0.001)	1.916 (0.002)	1.934 (0.002)	3.4 (0.2)			

^aGa doped.

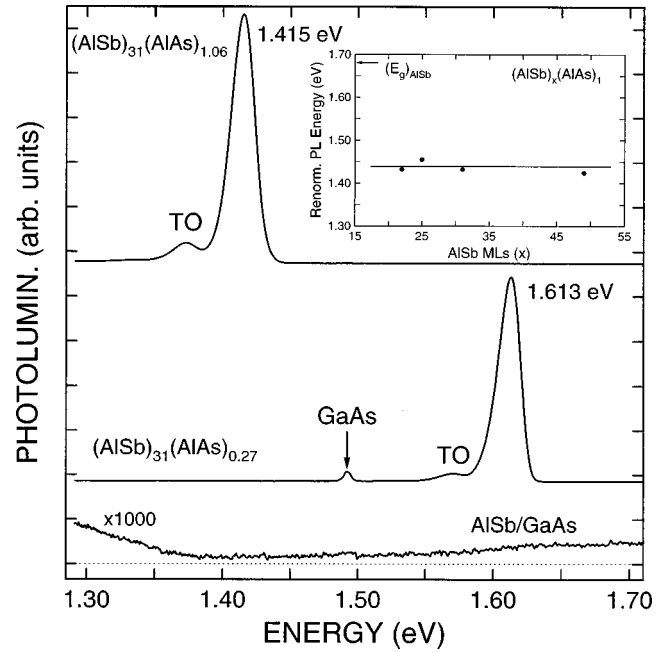


FIG. 2. PL spectra obtained at 1.6 K from the $(\text{AlSb})_{31}\text{AlAs}_{1.06}$ and $(\text{AlSb})_{31}(\text{AlAs})_{0.27}$ SL's and from the AISb/GaAs epitaxial film under 2.8 W/cm^2 of 488-nm radiation. The strong PL at 1.613 eV from the $(\text{AlSb})_{31}(\text{AlAs})_{0.27}$ SL excites the underlying GaAs substrate/buffer layer recombination at 1.49 eV. Inset: PL energy, normalized to 1 ML of AlAs, as a function of the AISb layer thickness. The line is a guide to the eye.

Several features are evident. First, the As planes induce very strong emission not observed in epitaxial AISb. In particular, a band at 1.415 eV was found for the $(\text{AlSb})_{31}(\text{AlAs})_{1.06}$ SL, and emission with a similar energy was found for the undoped SL's with 22 and 49 ML of AISb (see Table I). Similar PL was observed from the Ga- and Be-doped SL's. Second, the PL exhibits a strong dependence on the AlAs layer thickness. This is seen by the shift of the PL band to higher energy by $\sim 170\text{ meV}$ for the SL composed of 0.27 ML of AlAs and 31 ML of AISb. A weak dependence of the emission on the SL period is revealed after normalization of the PL to 1 ML of AlAs (inset in Fig. 2) by using a linear extrapolation between the PL energies found for the $(\text{AlSb})_{31}(\text{AlAs})_{1.06}$ and $(\text{AlSb})_{31}(\text{AlAs})_{0.27}$ SL's. Third, the strong PL bands occur at energies lower than the band gaps of AISb (1.7 eV) and AlAs (2.2 eV). Fourth, the small peak observed at 42 meV below the dominant emission can be understood as a TO (AISb) replica based on phonon energies

reported in the literature for bulk AlSb (Ref. 7). The much higher intensity of the zero phonon lines compared to that of the TO sideband suggests relaxation of the indirect character from the breaking of the translational invariance by the As planes. Fifth, the emission from the AlSb reference sample was extremely weak, typical of undoped epitaxial AlSb.

B. ODMR

ODMR was performed to determine the symmetry properties and hyperfine interactions of the recombining electron and hole. The magnetic-resonance results are best understood from recombination between an overlapping electron and hole at a superlattice interface. The overlap results in lifetimes ≥ 100 ns and weak-exchange coupling between the electron and hole spins.

The ODMR spectra were analyzed with the following spin Hamiltonian to describe the electronic states in a magnetic field for an electron and a (heavy) hole with a small-exchange interaction:³

$$H = \mu_B g_e \mathbf{S} \cdot \mathbf{B} + \mu_B g_h \mathbf{J} \cdot \mathbf{B} + \mathbf{aJ} \cdot \mathbf{S}, \quad (1)$$

where the first term is the Zeeman term for an electron with spin $= \frac{1}{2}$, the second term is the Zeeman term for a hole with spin $J = \frac{3}{2}$, μ_B is the Bohr magneton, g_e and g_h are the electron and hole (Zeeman) g values, and the last term describes the electron-hole exchange with strength \mathbf{a} . For the experiments to be discussed, the magnetic field is large enough that the Zeeman terms dominate.

Due to the strain in the AlSb layers, the $J = \frac{3}{2}$ valence band (VB) is split into $J_z = \pm \frac{3}{2}$ (heavy-hole) and $J_z = \pm \frac{1}{2}$ (light-hole) doublets. Under these conditions, the g values for holes associated with the $J_z = \pm \frac{3}{2}$ VB are highly anisotropic with $g_{\parallel} \sim 2-4$ and $g_{\perp} \sim 0$ (Ref. 8).

The ODMR from the $[(\text{AlSb})_{31}(\text{AlAs})_{1.06}]_{120}$ SL for several orientations of \mathbf{B} in the $(1\bar{1}0)$ plane is shown in Fig. 3. Several features are evident. First, three luminescence-increasing resonances are observed for $\mathbf{B} \parallel [001]$. Second, the splitting between the outer lines increases as \mathbf{B} approaches $[001]$. Third, the peak intensity of the low-field line is ~ 3 times that of the high-field line. Fourth, the middle resonance exhibits a small anisotropy with $(B_{\text{res}})_{[001]} > (B_{\text{res}})_{[110]}$. Finally, the intensities of the individual signals decrease as \mathbf{B} is rotated from $[001]$ to $[110]$. Overall, the present ODMR is very similar to that found on excitonic recombination from type-II short-period GaAs/AlAs MQW's.³⁻⁵ In that system, the recombination involves $S = \pm \frac{1}{2}$ electrons associated with the X-point conduction band minima in AlAs and $J_z = \pm \frac{3}{2}$ holes associated with the Γ -point VB maximum in GaAs.

The resonance positions vs magnetic-field orientation are plotted in Fig. 4. A fit to the data was made using the electron Zeeman and exchange terms of the spin Hamiltonian. Two main points are emphasized. First, the dependence of the splitting on angle ($\cos \theta$) provides strong evidence that the electron is coupled to a hole from the $J_z = \pm \frac{3}{2}$ VB with $g_{\perp} \sim 0$. Second, the two outer lines can be ascribed to electron spin transitions with $g_{\parallel} = 1.922 \pm 0.002$ and $g_{\perp} = 1.939 \pm 0.002$ split by an exchange interaction ($\Delta = a/2$) of $3.7 \pm 0.2 \mu\text{eV}$ with the hole. Most noteworthy, these g values lie between those reported for the X-point electrons in AlAs (Refs. 3-5 and 9) and AlSb (Ref. 9). In particular, the g

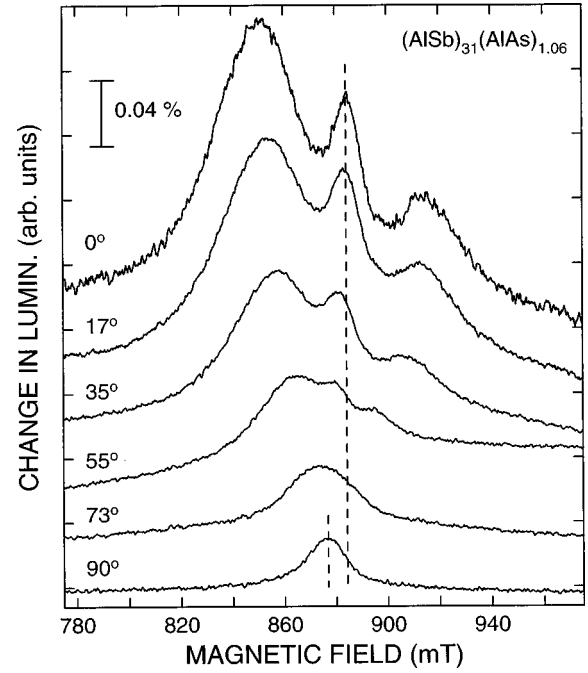


FIG. 3. ODMR spectra found at 24 GHz on the 1.415-eV emission from the $(\text{AlSb})_{31}(\text{AlAs})_{1.06}$ SL as a function of the angle between \mathbf{B} and the $[001]$ axis. Dashed lines indicate the small anisotropy in the peak position of the middle resonance.

values for Si donors in AlAs epitaxial layers are $g_{\perp} = 1.976 \pm 0.001$ and $g_{\parallel} = 1.917 \pm 0.001$ (with respect to the long axis of an X-valley ellipsoid)⁹ and for exchange-split electrons found on excitonic emission from type-II GaAs/AlAs MQW's are $g_{\perp} = 1.975 \pm 0.005$ and $g_{\parallel} = 1.895 \pm 0.005$ (Refs.

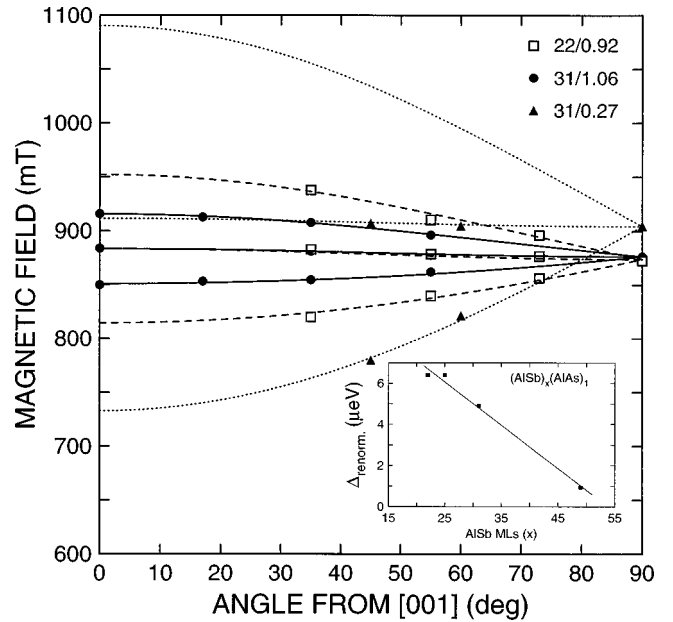


FIG. 4. Resonance fields vs magnetic-field orientation for three samples. Open squares $(\text{AlSb})_{22}(\text{AlAs})_{0.92}$ SL; closed circles, $(\text{AlSb})_{31}(\text{AlAs})_{1.06}$ SL; closed triangles, $(\text{AlSb})_{31}(\text{AlAs})_{0.27}$ SL. Curves are fits to the data using the spin Hamiltonian given in Eq. (1). Inset: Exchange-splitting energy (Δ_{renorm}), normalized to 1 ML of AlAs, as a function of the AlSb layer thickness. The line is a guide to the eye.

3–5). In addition, the g value reported for the singlet (a_1) ground state of Te donors in AISb is 1.883 ± 0.005 from magnetic resonance¹⁰ and ~ 1.90 using expressions for g_{\parallel} and g_{\perp} derived by Roth¹¹ from perturbation theory. Thus, the mixed AIAs/AISb character of the g values found for the (AISb)₃₁(AIAs)_{1.06} SL strongly suggests that a significant fraction of the electron wave function lies at the AIAs ML, with some penetration into the adjacent AISb layers.

The middle resonance in Fig. 3 can also be fit with the same g tensor used to describe the exchange-split electron resonances (see Fig. 4). The feature is distinguished by its different modulation-frequency dependence compared to that found for the exchange-split lines. This line may arise from spin-flip transitions of free electrons where the spin dependence is in the feeding of the strong recombination¹² or to electrons where the exchange coupling with the recombining holes is negligible.⁵

Similar ODMR was found on the PL from the undoped (AISb)₂₂(AIAs)_{0.92} (open squares in Fig. 4) and (AISb)₄₉(AIAs)_{0.88} SL's and from the Ga-doped (AISb)₂₅(AIAs)_{0.95} sample. The electron g values and exchange splittings are summarized in Table I. The g values vary slightly, while a much larger spread is found in the strength of the exchange interaction (3.4–8.0 μeV). The larger exchange splitting indicates a higher degree of overlap between the electron and hole wave functions.

The ODMR on the 1.62-eV band from the (AISb)₃₁(AIAs)_{0.27} SL only revealed evidence for two resonances (closed triangles in Fig. 4). The first exhibited a similar field-orientation dependence as that of the low-field ODMR found from the SL's with ~ 1 ML of AIAs. The second is slightly anisotropic, analogous to the behavior of the middle resonance observed for the samples discussed above. Following the analysis described above, this ODMR is assigned to $S = \frac{1}{2}$ electron spin transitions with $g_{\parallel} = 1.868 \pm 0.002$ and $g_{\perp} = 1.882 \pm 0.002$ split by an exchange interaction of $19.5 \pm 0.5 \mu\text{eV}$ with holes derived from the $J_z = \pm \frac{3}{2}$ VB. The slightly anisotropic line can again be fit with the same g tensor. These g values are very similar to those reported for shallow donors/conduction electrons in AISb (Ref. 10).

We note that the high-field branch of the exchange-split electron ODMR is not observed for the SL with 0.27 ML of AIAs. The absence of this line and the reduced intensity of the high-field exchange-split electron resonance relative to that of the low-field line from the SL's with ~ 1 ML of AIAs (e.g., see Fig. 3) are ascribed to thermalization effects that alter the relative populations of the four excited states.

In order to separate the effects due to the AIAs layer thickness and the SL period, we have plotted the exchange splittings as a function of the AISb layer thickness (inset in Fig. 4) after normalization of Δ to 1 ML of AIAs by using a linear extrapolation between the splittings found for the (AISb)₃₁(AIAs)_{1.06} and (AISb)₃₁(AIAs)_{0.27} SL's as was done for the PL energies. Most noteworthy, the exchange coupling decreases monotonically with increasing AISb layer thickness, in contrast to the behavior observed for the energies of the corresponding PL bands.

Finally, the hole spins in the AISb layers of the SL's are expected to be strongly oriented along the [001] axis due to the in-plane biaxial compression revealed by the x-ray stud-

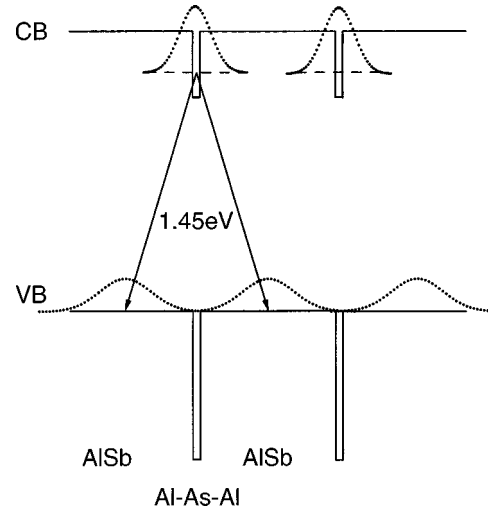


FIG. 5. Schematic diagram of proposed band structure for As monolayers embedded in AISb. Dotted curves illustrate the electron and hole wave functions.

ies. The strain lifts the fourfold degeneracy of the $J = \frac{3}{2}$ VB such that only states derived from the $J_z = \pm \frac{3}{2}$ VB are populated at 1.6 K. Preliminary wide-field scans on the (AISb)₃₁(AIAs)_{1.06} SL reveal an anisotropic resonance with $g_{\parallel} = 2.8 \pm 0.1$ and $g_{\perp} \sim 0$, consistent with the g tensor expected for holes derived from the $J_z = \pm \frac{3}{2}$ VB.

IV. DISCUSSION

The salient features of the PL data are the strong emission for As planes, the weak dependence of the emission on the SL period, and the strong dependence on AIAs ML thickness. The ODMR reveals an electron with AIAs ML and AISb barrier character coupled to a $J_z = \pm \frac{3}{2}$ hole. This character indicates that the hole is in the AISb layers. These features lead to a model for the recombination as an exciton bound at the As monolayer. Using the band offsets for AISb and AIAs (Ref. 6), the wave functions for the electron and hole are sketched in Fig. 5. There are three binding energies associated with this exciton. The electron is strongly bound at the plane—this binding determines the PL energy. The electron and hole are bound to form the exciton—this binding is reflected in the exchange. Finally, the exciton is localized at a fluctuation in the ML—this localization provides the width of the PL line (~ 20 meV). The exciton can also be viewed as bound at an isoelectronic plane.¹³

Strong recombination with similar linewidths has been reported for fractional and single monolayers of InAs embedded in GaAs (Refs. 14 and 15) and for CdSe in ZnSe (Ref. 16). For the InAs/GaAs system, the PL was attributed to excitonic recombination between electrons and holes bound at the InAs layers. The recombination for InAs single ML's was modeled using tight-binding calculations.¹⁴

The similarity of the PL bands from the Be- and Ga-doped SL's with those from the undoped structures indicates that these impurities do not compete favorably with the As planes for the photoexcited carriers. Furthermore, it appears that the strong PL bands observed from the AISb/AIAs SL's do not involve the donorlike defects produced by the “As-soak” technique. It was proposed that the unknown donors

may derive from As_{Al} antisite defects.¹ However, a four-line ODMR signal that arises from a central hyperfine interaction between the defect electron with spin $S = \frac{1}{2}$ and the As nucleus with spin $I = \frac{3}{2}$ was not found on this emission. It is possible that the donors may be involved in the weak infrared bands also observed from these test structures. ODMR on this PL is underway and will be discussed in a future paper.

V. SUMMARY

Superlattices composed of planes of As separated by 22–49 ML of AlSb were studied by photoluminescence and optically detected magnetic resonance. Very strong PL bands were found. The emission exhibits a strong dependence on the amount of As but a weak dependence on the SL period. The ODMR reveals $S = \frac{1}{2}$ electron-spin transitions, with g

values similar to those reported for X-point electrons in AlSb and AlAs, split by an exchange interaction (Δ) of 3.4–19.5 μeV with $J_z = \pm \frac{3}{2}$ holes. The results can be understood from a type-II band structure with the electron localized at the AlAs ML (with some wave-function penetration into the AlSb) and the hole excluded to the AlSb layers. The recombination is assigned to excitons weakly localized at fluctuations along the AlSb/AlAs interfaces. It appears that this emission does not involve the donorlike defects produced by the “As-soak” technique.

ACKNOWLEDGMENT

This work was supported by the Office of Naval Research.

-
- ¹G. Tuttle, H. Kroemer, and J. H. English, *J. Appl. Phys.* **67**, 3032 (1990).
- ²J. B. Boos, W. Kruppa, D. Park, B. V. Shanabrook, and B. R. Bennett, *Electron. Lett.* **30**, 1983 (1994); J. B. Boos, W. Kruppa, B. R. Bennett, D. Park, S. W. Kirchoefer, R. Bass, and H. B. Dietrich, *IEEE Trans. Electron Devices* **45**, 1869 (1998).
- ³H. W. van Kesteren, E. C. Cosman, and W. A. J. A. van der Poel, *Phys. Rev. B* **41**, 5283 (1990).
- ⁴J. M. Trombetta, T. A. Kennedy, D. Gammon, B. V. Shanabrook, and S. M. Prokes, *Mater. Sci. Forum* **83-87**, 1361 (1991).
- ⁵P. G. Baranov, I. V. Mashkov, N. G. Romanov, P. Lavallard, and R. Planel, *Solid State Commun.* **87**, 649 (1993).
- ⁶W. A. Harrison and J. Tersoff, *J. Vac. Sci. Technol. B* **4**, 1068 (1986).
- ⁷G. Hofmann, C. T. Lin, E. Schönherr, and J. Weber, *J. Appl. Phys.* **67**, 1478 (1990).
- ⁸See, e.g., E. Glaser, J. M. Trombetta, T. A. Kennedy, S. M. Prokes, O. J. Glembocki, K. L. Wang, and C. H. Chern, *Phys. Rev. Lett.* **65**, 1247 (1990), and references therein.
- ⁹E. R. Glaser, T. A. Kennedy, B. Molnar, R. S. Sillmon, M. G. Spencer, M. Mizuta, and T. F. Kuech, *Phys. Rev. B* **43**, 14 540 (1991), and references therein.
- ¹⁰W. Wilkening, U. Kaufmann, J. Schneider, E. Schönherr, E. R. Glaser, B. V. Shanabrook, J. R. Waterman, and R. J. Wagner, *Mater. Sci. Forum* **83-87**, 793 (1992).
- ¹¹L. M. Roth, *Phys. Rev.* **118**, 1534 (1960).
- ¹²C. Weisbuch and C. Herman, *Phys. Rev. B* **15**, 816 (1977).
- ¹³H. P. Hjalmarson, *J. Vac. Sci. Technol.* **21**, 524 (1982).
- ¹⁴A. R. Goñi, M. Stroh, C. Thomsen, F. Heinrichsdorff, V. Türck, A. Krost, and D. Bimberg, *Appl. Phys. Lett.* **72**, 1433 (1998), and references therein.
- ¹⁵K. Okamoto, T. Umezaki, T. Okada, and R. Shinohara, *Solid-State Electron.* **38**, 1335 (1995).
- ¹⁶S. V. Ivanov, A. A. Toropov, T. V. Shubina, S. V. Sorokin, A. V. Lebedev, I. V. Sedova, P. S. Kop'ev, G. R. Pozina, J. P. Bergman, and B. Monemar, *J. Appl. Phys.* **83**, 3168 (1998).